

CONCURRENT TARGET FOLLOWING WITH ACTIVE DIRECTIONAL SENSORS

Yiming Wang and Andrea Cavallaro

Centre for Intelligent Sensing, Queen Mary University of London
 {yiming.wang, a.cavallaro}@qmul.ac.uk

ABSTRACT

We propose a collision-avoidance tracker for agents with a directional sensor that aim to maintain a moving target in their field of view. The proposed tracker addresses the view maintenance issue within an Optimal Reciprocal Collision Avoidance (ORCA) framework. Our tracking agents adaptively share the responsibility of avoiding each other and minimise with a smooth actuation the deviation angle from their heading direction to their target. Experimental results with real people trajectories from public datasets show that the proposed method improves view maintenance.

Index Terms— Target following; active directional sensors; multi-agent systems; collision avoidance.

1. INTRODUCTION

A camera-equipped robot (agent) that autonomously follows a person in public places can provide various types of services or assistance. In public spaces, multiple agents may concurrently follow their target and therefore need to avoid collisions with other agents and targets (e.g. people). In multi-agent collision avoidance, *reciprocity* is important to avoid undesirable oscillations [1]. Reciprocity can be achieved when agents use the Optimal Reciprocal Collision Avoidance (ORCA) method [1, 2, 3, 4, 5, 6, 7, 8, 9]. With ORCA agents derive a set of velocities that will allow them to avoid collisions with nearby moving agents. Each agent then selects from this set the collision-free velocity that is the closest one to its preferred velocity (i.e. the velocity the agent would maintain in absence of obstacles). Moreover, for target following with a directional sensor, such as a camera, agents need to guarantee *view maintenance*, i.e. to keep the moving target at a certain distance and centred within the field of view (FoV). Therefore the collision-free velocities should further account for view maintenance, a constraint that - to the best of our knowledge - has not been explored in the literature yet.

In this paper we propose a view-maintenance method for collision avoidance manoeuvres. To enable smooth actuation when an agent heads towards its target, we adaptively set the feedback errors to compute the agent control from the collision-free velocity based on both the deviation angle and its derivative. Furthermore, we incorporate the relative risk of view loss to adapt the pair-wise responsibility so that agents whose risk of losing the view of their target is higher can reduce their share of responsibility and move more closely to their preferred velocity. We validate the proposed method with people trajectories extracted from publicly available datasets and demonstrate the improvements in view maintenance with the proposed method.

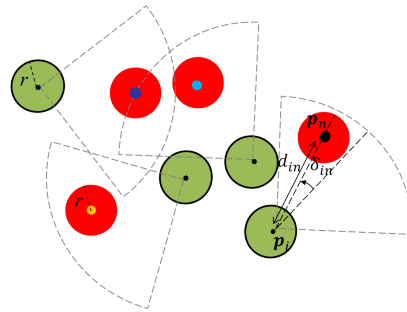


Fig. 1. Multiple agents (green) with a directional sensor follow their target (red). The goal of each agent is to maintain, despite the presence of multiple moving obstacles, its target at a certain desirable distance and viewing angle.

2. VIEW-AWARE CONCURRENT TARGET FOLLOWING

2.1. Preliminaries

Let multiple agents coexist in a shared area and let each agent follow one target at a time (Fig. 1). Each agent c_i is disk-shaped with radius r and position $\mathbf{p}_i(t)$ at time t . Each agent has a directional sensor with a sector-shaped FoV whose orientation is the same as the agent's heading direction.

Each target o_n is modelled as a disk of radius r and has position $\mathbf{p}_n(t)$ at time t . Let $d_{in}(t)$ be the distance between c_i and its target o_n at time t and $\delta_{in}(t) \in (-\pi, \pi]$ be the *deviation angle* from the agent heading direction to o_n (Fig. 1). Each c_i computes the control vector $\mathbf{u}_i(t)$ to maintain its target o_n at a certain desirable distance d_{in}^* in the agent's heading direction (i.e. $d_{in}(t) = d_{in}^*$ and $\delta_{in}(t) = 0$), while avoiding collisions with other agents and targets (i.e. $d_{ij}(t) > 2r, \forall j, j \neq i$ and $d_{in}(t) > 2r, \forall n$).

We assume that c_i knows which target to follow, receives (or infers) the preferred velocities of nearby agents and targets, and receives (or estimates) the positions of nearby agents and targets via an external tracker [2, 5] or via cooperative tracking [10, 11].

2.2. Collision-avoiding velocities

Let c_i and c_j at position \mathbf{p}_i and \mathbf{p}_j , respectively (to simplify the notation we will omit t), aim to achieve their respective *preferred velocity* \mathbf{v}_i^* and \mathbf{v}_j^* (Fig. 2(a)). Each agent c_i then exchanges its preferred velocity with neighbouring agents and derives the pair-wise velocity constraints induced by each of its neighbouring agents and targets using ORCA with adaptive responsibility sharing.

A *collision-free velocity*, \mathbf{v}_i^A , is obtained from which we compute a feasible control \mathbf{u}_i that minimises the deviation angle of the agent's heading direction from its target.

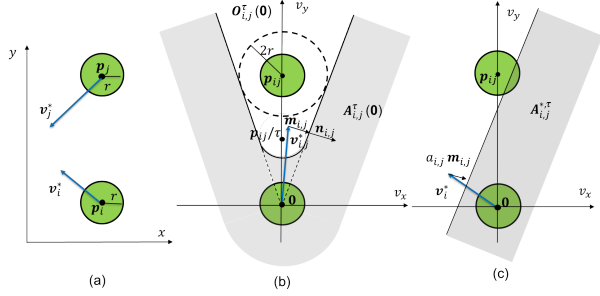


Fig. 2. Optimal reciprocal collision-avoiding velocities. (a) Agent c_i and c_j with radius r at \mathbf{p}_i and \mathbf{p}_j with their preferred velocity \mathbf{v}_i^* and \mathbf{v}_j^* , respectively. (b) The grey area indicates the relative velocities of c_i that are collision-avoiding with c_j in τ time steps ($\mathbf{A}_{i,j}^{\tau}(\mathbf{0})$). $\mathbf{m}_{i,j}$ is the minimal velocity for \mathbf{v}_i^* to get out of the velocity obstacle (starting from \mathbf{v}_i^* to the closest point at the boundary of the velocity obstacle). $\mathbf{n}_{i,j}$ is the outward normal. (c) The grey area indicates the velocities of c_i that are optimal reciprocal collision-avoiding with c_j in τ time steps ($\mathbf{A}_{i,j}^{*,\tau}$) by sharing $a_{i,j}$ responsibility to avoid c_j .

Let the target o_n of agent c_i be at \mathbf{p}_n with velocity \mathbf{v}_n . If v_{max} is the maximum agent speed, then we compute \mathbf{v}_i^* as:

$$\mathbf{v}_i^* = \mathbf{e}_{in} \max \left(\min \left((\tilde{d}_{in} - d_{in}^*)/T_o, v_{max} \right), -v_{max} \right), \quad (1)$$

where T_o is temporal interval during which the velocity will be maintained ($T_o = 1$ s when the velocity is maintained for one second), \tilde{d}_{in} is the distance between the position \mathbf{p}_i of agent c_i and the predicted target position $\tilde{\mathbf{p}}_n$ estimated using the current target velocity. \mathbf{e}_{in} is the unit vector indicating the direction from \mathbf{p}_i towards $\tilde{\mathbf{p}}_n$.

With knowledge of the preferred velocities of nearby agents and targets, each agent then derives the pair-wise velocity constraint induced by each its nearby agent and target. We first derive the Velocity Obstacle (VO) of c_i induced by c_j , i.e. the set of velocities of c_i that can lead to a collision with c_j in a time horizon τ [12]. In the relative velocity space of c_j (as shown in Fig. 2(b)), let $\mathbf{O}_{i,j}^{\tau}(\mathbf{0})$ be the VO of c_i induced by c_j assuming that c_j moves at its preferred velocity, i.e. $\mathbf{0}$:

$$\mathbf{O}_{i,j}^{\tau}(\mathbf{0}) = \{ \mathbf{v} \mid \|\mathbf{v}\| \geq \|\mathbf{p}_{ij} - 2r\|, t \in [0, \tau] \}, \quad (2)$$

where \mathbf{p}_{ij} is the relative position of c_j with respect to c_i . The set of collision-avoiding relative velocities for c_i to avoid c_j in τ time horizon, $\mathbf{A}_{i,j}^{\tau}(\mathbf{0})$, can be therefore represented as $\mathbf{A}_{i,j}^{\tau}(\mathbf{0}) = \{ \mathbf{v} \mid \mathbf{v} \notin \mathbf{O}_{i,j}^{\tau}(\mathbf{0}) \}$.

Reciprocal collision avoidance is possible when c_i and c_j choose to move at $\mathbf{v}_i \in \mathbf{A}_{i,j}^{\tau}(\mathbf{v}_j)$ and $\mathbf{v}_j \in \mathbf{A}_{j,i}^{\tau}(\mathbf{v}_i)$, respectively [1]. When \mathbf{v}_i^* lies within the VO as shown in Fig. 2(b), ORCA shifts \mathbf{v}_i^* out of the VO with a minimal effort that is contributed by both agents.

Let $\mathbf{m}_{i,j}$ be the minimal relative velocity change to avoid collisions. Therefore $\mathbf{m}_{i,j}$ is the vector starting from \mathbf{v}_i^* to the closest point at the boundary of the VO. $\mathbf{n}_{i,j}$ is the plane normal at $\mathbf{v}_i^* + \mathbf{m}_{i,j}$ with the direction pointing outside the VO.

2.3. Adaptive responsibility

Agents share the responsibility for avoiding a collision. Let $a_{i,j}$ and $a_{j,i}$ be the responsibility shared by c_i and c_j to avoid each other and

$a_{i,j} + a_{j,i} = 1$. The set of optimal reciprocal collision-avoiding velocity for c_i to avoid c_j in τ time steps is defined as:

$$\mathbf{A}_{i,j}^{*,\tau} = \{ \mathbf{v} \mid \mathbf{v} - (\mathbf{v}_i^* + a_{i,j} \mathbf{m}_{i,j}) \cdot \mathbf{n}_{i,j} \leq 0 \}. \quad (3)$$

As shown in Fig. 2(c), $\mathbf{A}_{i,j}^{*,\tau}$ are the velocities in the grey half-plane at the direction of $\mathbf{n}_{i,j}$. The set of collision-avoiding velocities of c_j induced by c_i , i.e. $\mathbf{A}_{j,i}^{*,\tau}$, can be constructed in the same way.

Let $\mathbf{A}_{i,n}^{*,\tau}$ be the set of velocities of c_i that are collision-avoiding with o_n in τ time steps. If \mathbf{C}_i^A and Λ_i^A are the set of agents and targets within the avoidance range, then the set of accessible velocities of c_i that are collision-avoiding with all agents and targets is:

$$\mathbf{A}_i^{*,\tau} = \left(\bigcap_{c_j \in \mathbf{C}_i^A} \mathbf{A}_{i,j}^{*,\tau} \right) \cap \left(\bigcap_{o_n \in \Lambda_i^A} \mathbf{A}_{i,n}^{*,\tau} \right) \cap \mathbf{V}_i, \quad (4)$$

where \mathbf{V}_i is the set of accessible velocities under speed/acceleration limits.

The new collision-free velocity \mathbf{v}_i^A lies within $\mathbf{A}_i^{*,\tau}$ and is the closest to \mathbf{v}_i^* . Note that $\mathbf{A}_i^{*,\tau} = \emptyset$ can occur when c_i is densely surrounded by agents or targets. This problem can be addressed by allowing the agent to intrude slightly the velocity constraints until at least one accessible velocity is found [1].

The choice of the pair-wise responsibility influences the number and distribution of the accessible collision-free velocities of the pair of agents [13, 14]. Unlike [1, 2, 5, 15, 16] that share the responsibility equally, we adapt the responsibility based on the risk of an agent losing its target, which can be measured as velocity difference, $\Delta \mathbf{v}_i^*$, between the preferred velocity \mathbf{v}_i^* and the current velocity \mathbf{v}_i .

Let q_i be the risk of c_i losing its target. We compute this risk as $q_i = e^{\|\Delta \mathbf{v}_i^*\|}$. The responsibility $a_{i,j}$ that c_i shares with c_j depends on the difference between q_i and q_j . To obtain a continuous and bounded value we adopt the Jain's fairness measure to quantify how alike two values are [17]. The fairness, ϱ_{ij} , between q_i and q_j is:

$$\varrho_{ij} = \frac{1}{2} \frac{(q_i + q_j)^2}{q_i^2 + q_j^2}, \quad (5)$$

where $\varrho_{ij} \in [0.5, 1]$, with $\varrho_{ij} = 0.5$ being the least fair case and $\varrho_{ij} = 1$ being the fairest case.

We finally compute the responsibility for c_i to avoid c_j , $a_{i,j}$, as:

$$a_{i,j} = \begin{cases} \varrho_{ij} - 0.5 & q_i > q_j \\ 1.5 - \varrho_{ij} & q_i \leq q_j \end{cases}, \quad (6)$$

where the two constants 0.5 and 1.5 ensure that $a_{i,j} \in [0.5, 1]$. We then compute in the same way the responsibility $a_{j,i}$ for c_j to avoid c_i .

2.4. Minimisation of the deviation angle

Each agent computes a feasible control from \mathbf{v}_i^A . Let \mathbf{p}_i^A be the temporary goal position of c_i set by \mathbf{v}_i^A (Fig. 3). Let $\varphi_i^A \in (-\pi, \pi]$ be the angle from the agent's heading direction to \mathbf{p}_i^A . It is common to compute the control \mathbf{u}_i based on the feedback of the distance error, $d_{i,e}$, between \mathbf{p}_i and \mathbf{p}_i^A and the angle error, $\varphi_{i,e}$, from current agent's heading to \mathbf{p}_i^A . The agent can either move forward, i.e. positive $d_{i,e}$, while turning φ_i^A to the right side of the agent, or move backward, i.e. negative $d_{i,e}$, while turning the complement angle of φ_i^A to the left side of the agent. Works on multi-agent navigation set $d_{i,e}$ positive [4, 5, 15, 18] as the agent's heading is of little importance, while we minimise the deviation angle δ_{in} by properly

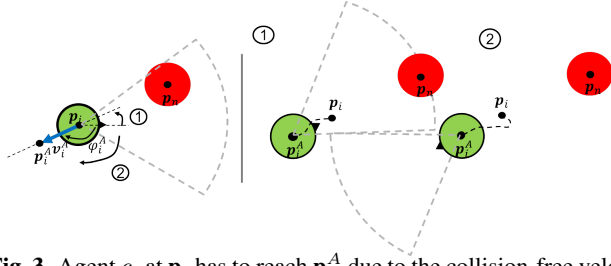


Fig. 3. Agent c_i at \mathbf{p}_i has to reach \mathbf{p}_i^A due to the collision-free velocity \mathbf{v}_i^A . φ_i^A is the angle from the agent's heading to \mathbf{p}_i^A . Two options can reach \mathbf{p}_i^A but Option 2 results in a view loss.

setting the sign of $d_{i,e}$ in order to avoid unnecessary view loss on targets (Option 2 in Fig. 3).

Let $d_{i,e}^+$ and $\varphi_{i,e}^+$ be the distance error and the angular error of a forward movement, respectively, that can be computed as:

$$\begin{aligned} d_{i,e}^+ &= \left\| \mathbf{v}_i^A \right\| \\ \varphi_{i,e}^+ &= \varphi_i^A. \end{aligned} \quad (7)$$

Correspondingly, $d_{i,e}^-$ and $\varphi_{i,e}^-$ are the distance and angular error of a backward movement:

$$\begin{aligned} d_{i,e}^- &= - \left\| \mathbf{v}_i^A \right\| \\ \varphi_{i,e}^- &= \varphi_i^A - \text{sign}(\varphi_i^A)\pi. \end{aligned} \quad (8)$$

We compute the candidate control vectors of the two options using the feedback-based method in [19]. Let X be either + or - and $\mathbf{u}_i^X = [v_i^X, \omega_i^X]$ be the control vector with v_i^X for the speed control and ω_i^X for the steering control. The resulted deviation angle in ΔT time, $\delta_{in}^X(\Delta T)$, given the control \mathbf{u}_i^X can then be computed as $\delta_{in}^X(\Delta T) = \delta_{in} + \Delta\delta_{in}^X$, where $\Delta\delta_{in}^X$ is the difference of the deviation angle between two consecutive time steps. When agents follow a differential-drive kinematic model then

$$\Delta\delta_{in}^X = -\omega_i^X \Delta T + \frac{v_i^X \Delta T}{d_{in}} \sin(\delta_{in}). \quad (9)$$

To minimise the deviation angle, one can select the direction of movement (forward or backward) that leads to a smaller $|\delta_{in}(\Delta T)|$. However, oscillations can occur due to direction flipping when the target direction is orthogonal to \mathbf{v}_i^A . To address this problem and achieve smooth motion, we first select a candidate movement direction that leads to a smaller $|\Delta\delta_{in}|$. If the resulting $|\Delta\delta_{in}(\Delta T)| > \frac{\pi}{2}$, i.e. the agent heading opposite to its target, the direction with a smaller $|\delta_{in}(\Delta T)|$ is selected. Otherwise, the candidate movement direction is the final movement direction and the corresponding control vector is used to update the agent's state, i.e. the position and heading direction.

3. VALIDATION

We compare Differential-Drive agents moving with DD-AR-DM, the proposed method using Adaptive Responsibility sharing and Deviation angle Minimisation, against DD-AR, the same method using only Adaptive Responsibility sharing, and DD-DM, using only Deviation angle Minimisation, as well as DD, Snape's method [5]. We base the implementation on the RVO2¹ library.

¹<http://gamma.cs.unc.edu/RVO2>. Last accessed: 27/10/2017

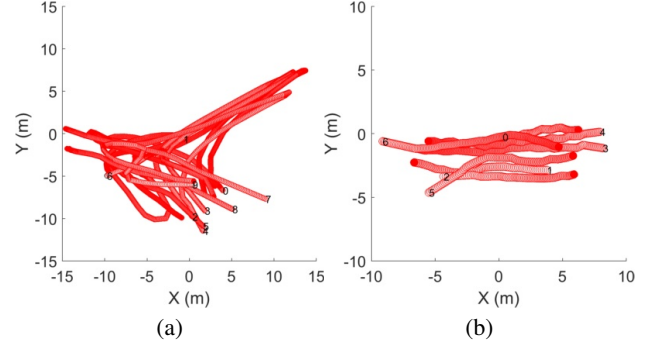


Fig. 4. Trajectories of Scenario (a) I and (b) II. Numbers are the indices and starting positions of targets. The red intensity increases over time.

Targets are initialised at the agent's heading direction at the desired agent-target distance, $d_{in}^* = 2\text{m}$. The maximum speed of the agents is $v_{\max} = 2\text{m/s}$. The maximum speed of targets is smaller than that of the agents to guarantee the capture of targets. The agent avoidance range is set to $2v_{\max}$, which is the worst case for a collision between a pair of agents in one second. We set the time horizon $\tau = 3$ for a moderate avoidance aversion [2]. The radius of agents and targets, r , is 0.3m and is set to 0.6m when deriving the velocity constraints to compensate for tracking errors [5].

We consider two scenarios. Scenario I is a $30\text{m} \times 30\text{m}$ area with 10 trajectories of 60s from S2L1 sequence of the PETS2009 dataset². The sequence contains people walking with various patterns, such as meeting and random walking (Fig. 4 (a)). Scenario II is a $20\text{m} \times 20\text{m}$ area with 7 trajectories of 16s from the ETH Walking Pedestrian Hotel sequence³. The sequence contains the trajectories of two groups of pedestrians intersecting each other from opposite directions (Fig. 4 (b)).

As performance measures we consider deviation angle and distance maintenance. The *deviation angle*, η_i^δ , is measured as percentage of simulation time T during which the absolute value of the deviation angle from the agent heading towards its target is smaller than an error bound δ^E :

$$\eta_i^\delta = \frac{1}{T} \sum_{t=1}^T |\delta_{in}(t)| \leq \delta^E. \quad (10)$$

The *distance maintenance*, η_i^d , is measured as percentage of simulation time T during which the difference between the actual agent-target distance and the desired distance is smaller than an error bound d^E :

$$\eta_i^d = \frac{1}{T} \sum_{t=1}^T |d_{in}(t) - d_{in}^*| \leq d^E. \quad (11)$$

As the choice of the deviation angle error bound δ^E and the distance error bound d^E influences the view maintenance results, we perform the evaluation with varying error bound values: $\delta^E \in [0^\circ, 90^\circ]$ with a 9° step; and $d^E \in [0, 1]\text{m}$ with a 0.1m step.

Fig. 5 shows the average deviation angle performance and the distance maintenance performance for all agents in Scenario I and II. Adaptive responsibility sharing (DD-AR) outperforms DD in maintaining the agent-target distance regardless of the value of d^E , but

²<http://www.cvg.reading.ac.uk/PETS2009>. Last accessed: 27/10/2017

³<http://www.vision.ee.ethz.ch/en/datasets>. Last accessed: 27/10/2017

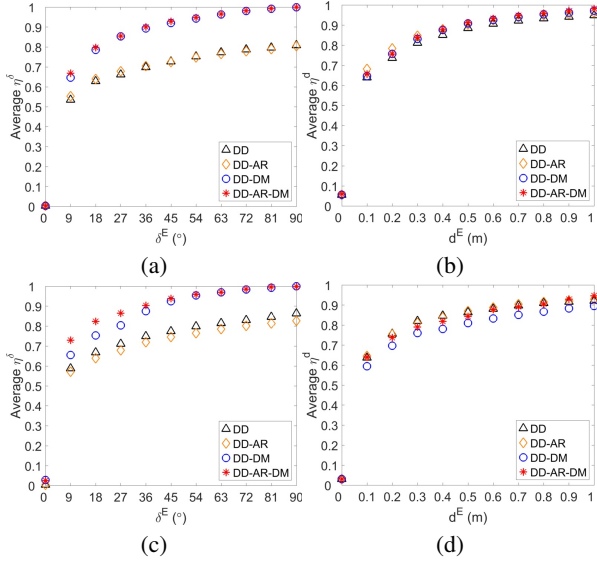


Fig. 5. Performance at various δ^E and d^E . Scenario I: (a) average deviation angle maintenance and (b) average distance maintenance; Scenario II: (c) average deviation angle maintenance and (d) average distance maintenance.

not in maintaining the deviation angle. DD computes the control from the collision-free velocity only accounting for forward motions, which easily causes the agent to head opposite to its target when the collision-free velocity is backwards or people move back and forth. DD-DM improves the deviation angle performance of DD. The average deviation angle ratio of DD-DM reaches 100% at $\delta^E = 90^\circ$, as the algorithm avoids the agent heading opposite to its target, i.e. when the absolute deviation angle is larger than 90° . This can be observed from Fig. 6, which shows the deviation angle and the agent-target distance of agent 6 that experiences frequent backward collision-free velocities in Scenario I.

DD-DM maintains the deviation angle at the cost of a reduced distance maintenance performance, because DD-DM forces the agent to head towards its target, which can cause an agent deviate from its desired agent-target distance due to the adjustments of agent heading. On the other hand, by adding the adaptive responsibility sharing to DD-DM, i.e. DD-AR-DM, the best deviation angle maintenance performance is achieved regardless of the value of δ^E . Moreover, DD-AR-DM improves the distance maintenance performance compared to DD-DM, but not compared to DD-AR.

On average, DD-AR-DM improves the deviation angle by 26% and 20% compared to DD in Scenario I and Scenario II, respectively. The performance improvement on the deviation angle in Scenario I is higher than that in Scenario II where the trajectories have forward motion only, while in Scenario I people also turn backwards.

Fig. 7 shows snapshots of agents' trajectories in Scenario I with DD and DD-AR-DM at the time step 310. We observe that with DD agent 2 and 3 head opposite to their target when the targets are turning back (Fig. 7(a)), whereas with DD-AR-DM, agent 2 and 3 can maintain their heading direction towards their target (Fig. 7(b)). Similar behaviour exists when the collision-free velocity is backwards, for example, agent 0.

The average travel distance of agents with DD, DD-AR, DD-DM and DD-AR-DM in Scenario I are 28m, 28.5m, 24.2m and 25m, respectively, and in Scenario II are 15m, 15m, 16.5m and 15m, respectively. The deviation angle minimisation affects the travel

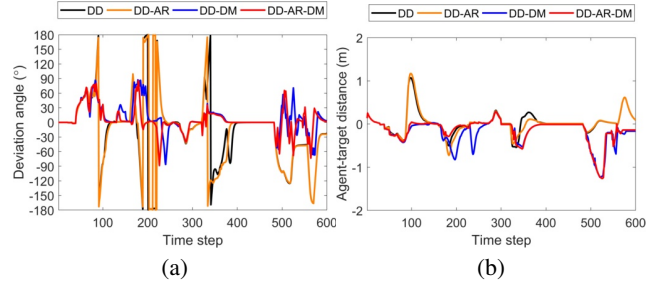


Fig. 6. Deviation angle (a) and agent-target distance (b) over time for agent 6 in Scenario I using different methods.

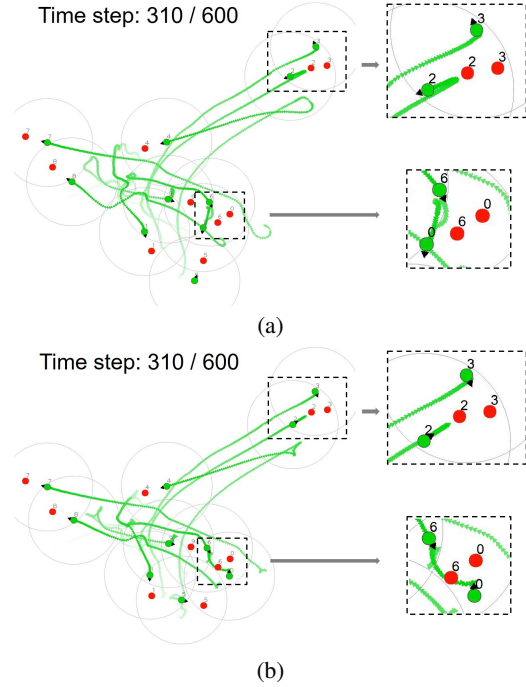


Fig. 7. Agent trajectories in Scenario I at time step 310 using (a) DD and (b) DD-AR-DM. Agents (green) follow their target with the same index (red). The heading direction of an agent is indicated by a triangle with increasing intensity over time. Circles indicate the collision avoiding range. Selected areas are magnified.

distance more than adaptive responsibility sharing. Demonstration videos can be found here⁴.

4. CONCLUSIONS

We proposed a target following method that accounts for view maintenance in terms of view angle and agent-target distance in an Optimal Reciprocal Collision Avoidance framework. To address the view maintenance objective during collision avoidance manoeuvres, the proposed algorithm adapts the pair-wise responsibility based on the relative risk for agents to lose their targets and minimises smoothly the agent deviation angle from its target when computing the feasible control. We validated the proposed method with real people trajectories. Future work will validate the proposed method on robotic platforms with real-time sensing, control and actuation.

⁴<http://www.eecs.qmul.ac.uk/~andrea/vorca.html>

5. REFERENCES

- [1] J. V. D. Berg, Guy Stephen J., Lin Ming, and Manocha Dinesh, "Reciprocal n-body collision avoidance," in *Proc. of Int'l Symp. on Robotics Research*, vol. 70, pp. 3–19. Springer, 2009.
- [2] D. Bareiss and J. V. D. Berg, "Generalized reciprocal collision avoidance," *Int'l J. of Robotics Research*, vol. 34, no. 12, pp. 1501–1514, Oct 2015.
- [3] J. Alonso-Mora, S. Baker, and D. Rus, "Multi-robot navigation in formation via sequential convex programming," in *Proc. of IEEE/RSJ Int'l Conf. on Intelligent Robots and Systems*, Hamburg, Germany, Sep 2015, pp. 4634–4641.
- [4] J. Snape, J. V. D. Berg, S. J. Guy, and D. Manocha, "Independent navigation of multiple mobile robots with hybrid reciprocal velocity obstacles," in *Proc. of IEEE/RSJ Int'l Conf. on Intelligent Robots and Systems*, St. Louis, USA, Oct 2009, pp. 5917–5922.
- [5] J. Snape, J. V. D. Berg, S. J. Guy, and D. Manocha, "Smooth and collision-free navigation for multiple robots under differential-drive constraints," in *Proc. of IEEE/RSJ Int'l Conf. on Intelligent Robots and Systems*, Taipei, Taiwan, Oct 2010, pp. 4584–4589.
- [6] H. Cheng, Q. Zhu, Z. Liu, T. Xu, and L. Lin, "Decentralized navigation of multiple agents based on orca and model predictive control," in *Proc. of IEEE/RSJ Int'l Conf. on Intelligent Robots and Systems*, Vancouver, Canada, Sept 2017, pp. 3446–3451.
- [7] S. Roelofsen, D. Gillet, and A. Martinoli, "Collision avoidance with limited field of view sensing: A velocity obstacle approach," in *Proc. of IEEE Int'l Conf. on Robotics and Automation*, Singapore, May 2017, pp. 1922–1927.
- [8] J. Alonso-Mora, E. Montijano, M. Schwager, and D. Rus, "Distributed multi-robot formation control among obstacles: A geometric and optimization approach with consensus," in *Proc. of IEEE Int'l Conf. on Robotics and Automation*, Stockholm, Sweden, May 2016, pp. 5356–5363.
- [9] J. Alonso-Mora, S. Baker, and D. Rus, "Multi-robot formation control and object transport in dynamic environments via constrained optimization," *Int'l J. of Robotics Research*, vol. 36, no. 9, pp. 1000–1021, 2017.
- [10] B. Beck and R. Baxley, "Anchor free node tracking using ranges, odometry, and multidimensional scaling," in *Proc. of IEEE Int'l Conf. on Acoustics, Speech and Signal Processing*, Florence, Italy, May 2014, pp. 2209–2213.
- [11] G. Ren, I. D. Schizas, and V. Maroulas, "Sparsity based multi-target tracking using mobile sensors," in *Proc. of IEEE Int'l Conf. on Acoustics, Speech and Signal Processing*, Shanghai, China, Mar 2016, pp. 4578–4582.
- [12] P. Fiorini and Z. Shillert, "Motion planning in dynamic environments using velocity obstacles," *Int'l Journal of Robotics Research*, vol. 17, pp. 760–772, 1998.
- [13] S. Curtis, B. Zafar, A. Gutub, and D. Manocha, "Right of way: Asymmetric agent interactions in crowds," *Visual Computer*, vol. 29, no. 12, pp. 1277–1292, 2013.
- [14] Y. Wang and A. Cavallaro, "Active visual tracking in multi-agent scenarios," in *Proc. of IEEE Int'l Conf. on Advanced Video and Signal-Based Surveillance*, Lecce, Italy, Sep 2017, pp. 1–6.
- [15] J. Alonso-Mora, A. Breitenmoser, P. Beardsley, and R. Siegwart, "Reciprocal collision avoidance for multiple car-like robots," in *Proc. of IEEE Int'l Conf. on Robotics and Automation*, Saint Paul, USA, May 2012, pp. 360–366.
- [16] J. Alonso-Mora, T. Naegeli, R. Siegwart, and P. Beardsley, "Collision avoidance for aerial vehicles in multi-agent scenarios," *Autonomous Robots*, vol. 39, pp. 101–121, Jan 2015.
- [17] R. Jain, D. Chiu, and W. Hawe, "A quantitative measure of fairness and discrimination for resource allocation in shared computer systems," *Computing Research Repository*, 1998.
- [18] J. Alonso-Mora, A. Breitenmoser, M. Ruffi, P. Beardsley, and R. Siegwart, "Optimal reciprocal collision avoidance for multiple non-holonomic robots," in *Proc. of Int'l Symposium on Distributed Autonomous Robotic Systems*, Lausanne, Switzerland, Nov 2010.
- [19] S. Lee, Y. Cho, M. H. Bo, B. You, and S. Oh, "A stable target-tracking control for unicycle mobile robots," in *Proc. of IEEE/RSJ Int'l Conf. on Intelligent Robots and Systems*, Takamatsu, Japan, Nov 2000, vol. 3, pp. 1822–1827.